Effect of Transmitter Position on the Torque Generation of a Magnetic Resonance Based Motoring system

Matthias Vandeputte
Dept. of Electrical Energy, Metals, Mechanical Constructions & Systems
Ghent University
9000 Ghent, Belgium
EEDT-DC, Flanders Make
matthias.vandeputte@UGent.be

Luc Dupré
Dept. of Electrical Energy, Metals, Mechanical Constructions & Systems
Ghent University
9000 Ghent, Belgium
luc.dupre@UGent.be

Guillaume Crevecoeur
Dept. of Electrical Energy, Metals, Mechanical Constructions & Systems
Ghent University
9000 Ghent, Belgium
EEDT-DC, Flanders Make
guillaume.crevecoeur@UGent.be

***Abstract*—Strongly coupled magnetic resonance is most often used to transfer electrical power from a transmitter to a resonant receiver coil to supply devices over an air gap. In this work, the induced current in two receiver coils (stator and rotor) is used to generate torque on the rotor coil. The effect of the transmitter position relative to the stator and rotor receiver coils on the torque generation is studied in detail, both in simulation and experimentally. Results show a 36% to 37% gain in peak torque when properly varying the stator orientation for a given transmitter distance.**

***Index Terms*—Wireless power transfer, magnetic resonance, energy conversion, coils, electromagnetic forces, mutual coupling, RLC circuits**

I. Introduction

Resonant wireless power transfer (RWPT) or strongly coupled magnetic resonance (SCMR) has been developed to transfer electrical energy over air gaps [1]–[6]. The current in one (transmitter) coil induces a voltage in another (receiver) coil when they are magnetically coupled. A capacitor can be connected in series with the coil to overcome its inductance, resulting in resonance. The principle of resonant coupling has been used for low to high power applications [7]–[11]. In previous research, SCMR was used to generate torque on a resonator coil [12], [13]. The current in a transmitter coil induces currents in two receiver resonators of which one is allowed to rotate around an axis. These induced currents then generate a torque on the rotor body, resulting in motoring behavior of the SCMR system.

The torque generating capability of the SCMR motoring system is highly dependent on multiple factors. First, the magnetic interaction between the fixed (stator) resonator and the rotating (rotor) resonator severely affect the resonant behavior of both coils. The induced currents in both coils tend to have their peak value when both resonators are not magnetically coupled. When they are coupled, frequency splitting occurs resulting in a local current minimum at the resonance frequency [14]. Secondly, the orientation of the transmitter with respect to the resonator pair presents a trade-off in two mechanisms that affect the torque generation. These are the magnetic coupling between transmitter and stator and the coupling between transmitter and rotor at the peak current position (no coupling between stator and rotor). Finally, the magnetic coupling between transmitter and receiver coils drops drastically when increasing the air gap, resulting in lower induced current. This paper researches the effect of the system geometry, and most importantly the transmitter position relative to the receiver coils, on the torque generating capability of a SCMR motoring system.

In Section II, the torque expressions are presented for a SCMR motoring system with a transmitter connected to a current of voltage controlled power source. The experimental setup is detailed in Section III-A, with validation of the torque expressions in Section III-B. A discussion on the effect of the transmitter position on the torque generation capability of the SCMR motoring system is presented in Section IV.

II. SCMR based motoring

In previous research [12], models were constructed to predict the induced resonator currents and the resulting torque in an SCMR system with one stator (s) and one rotor coil (r). It is shown that the torque is unidirectional under resonant conditions. The torque (T) can be described as a function of the current in the transmitter (t):

$$T(\theta) = \frac{1}{2}\frac{M_{ts}\omega^2(K_{sr}M_{tr} - K_{tr}M_{sr})}{\omega^2 M_{sr}^2 + R_r R_s}\mathrm{i}_t^2 \qquad (1)$$

with ω the electrical angular speed ($\omega = 2\pi f$), i_t the transmitter current amplitude, R_a the equivalent series resistance (ESR) of coil a and M_{ab} the mutual inductance between coils

Matthias Vandeputte holds a doctoral grant strategic basic research of the Fund for Scientific Research Flanders (FWO, project G0D9316N). The authors furthermore acknowledge the BOF (project 01N02716).

978-1-7281-3398-0/19/$31.00 ©2019 European Union

a and b. K_{ab} is the spatial derivative of mutual inductance $\left(K_{ab} = \frac{\mathrm{d}M_{ab}(\theta)}{\mathrm{d}\theta}\right)$. The torque can also be expressed as a function of the voltage over the transmitter:

$$T(\theta) = \frac{1}{2}\frac{M_{ts}\omega^2(K_{sr}M_{tr} - K_{tr}M_{sr})}{\omega^2 M_{sr}^2 + R_r R_s}\frac{\mathrm{v}_t^2}{|R_t + j\omega L_t + Z_r|^2} \tag{2}$$

with Z_r the reflected impedance of the stator and rotor resonator to the transmitter.

$$Z_r = \frac{\omega^2 M_{tr}^2 R_s + \omega^2 M_{ts}^2 R_r - 2j\omega^3 M_{sr} M_{tr} M_{ts}}{\omega^2 M_{sr}^2 + R_r R_s} \tag{3}$$

Filling in (3) in (2) results in expression (4):

$$T(\theta) = \frac{1}{2}\frac{M_{ts}\omega^2(K_{sr}M_{tr} - K_{tr}M_{sr})(\omega^2 M_{sr}^2 + R_r R_s)}{\left([R_t(\omega^2 M_{sr}^2 + R_r R_s) + \omega^2 M_{tr}^2 R_s + \omega^2 M_{ts}^2 R_r]^2 + [\omega L_t(\omega^2 M_{sr}^2 + R_r R_s) - 2\omega^3 M_{sr} M_{tr} M_{ts}]^2\right)}\mathrm{v}_t^2 \tag{4}$$

If we only consider the first spatial harmonic of the mutual inductance profiles (M_{tr} and M_{sr}), these can be expressed as:

$$\begin{aligned} M_{tr}(\theta) &= \mathbb{M}_{tr}\sin(\theta) \\ M_{sr}(\theta) &= \mathbb{M}_{sr}\sin(\theta - \phi_{st}) \\ K_{tr}(\theta) &= \mathbb{K}_{tr}\cos(\theta) = \mathbb{M}_{tr}\cos(\theta) \\ K_{sr}(\theta) &= \mathbb{K}_{sr}\cos(\theta - \phi_{st}) = \mathbb{M}_{sr}\cos(\theta - \phi_{st}) \end{aligned} \tag{5}$$

With $\mathbb{M}_{ab}$ the amplitude of the fist spatial harmonic of $M_{ab}(\theta)$. The mutual inductance profile M_{sr} is shifted by the angle ϕ_{st} compared to M_{tr}. This angle also corresponds to the stator orientation if the symmetry line of the coil coincides with the rotor axle. Equation (2) can now be simplified to:

$$T(\theta) = \frac{1}{2}\frac{\omega^2 M_{ts}\mathbb{M}_{tr}\mathbb{M}_{sr}\sin(\phi_{st})}{\omega^2\mathbb{M}_{sr}^2\sin(\theta - \phi_{st})^2 + R_r R_s}\frac{\mathrm{v}_t^2}{|R_t + j\omega L_t + Z_r|^2} \tag{6}$$

From (6) it is clear that the torque is unidirectional if only the first harmonic is considered. The sign of the torque is then only dependent on the stator orientation by the term $\sin(\phi_{st})$. This simplification is acceptable if the SCMR motoring system has enough symmetry and/or if the distance between the coils is large enough.

Based on (6) we would expect that the torque profile has a peak value when $\sin(\theta - \phi_{st}) = 0$, which corresponds to a zero magnetic coupling between stator and rotor. At this position, the reflected impedance to the transmitter (3) is purely resistive. The torque is higher for higher maximum coupling between all coils (M_{ts}, $\mathbb{M}_{tr}$ and $\mathbb{M}_{sr}$). The torque scales with $\sin(\phi_{st})$, but the mutual inductance between transmitter and stator (M_{ts}) also changes depending on the stator orientation.

III. Experimental Setup and Validation

A. Experimental setup

An experimental setup (Figure 1) was built to validate the torque profile expressions presented in Section II. This setup was also used in [12] to validate the general torque profile expressions. Since then, the setup was altered such that the transmitter position relative to the resonator pair can be changed, namely the transmitter distance (d) and stator orientation (ϕ_{st}) can be switched to three discrete positions. The considered system has one transmitter and stator coil with

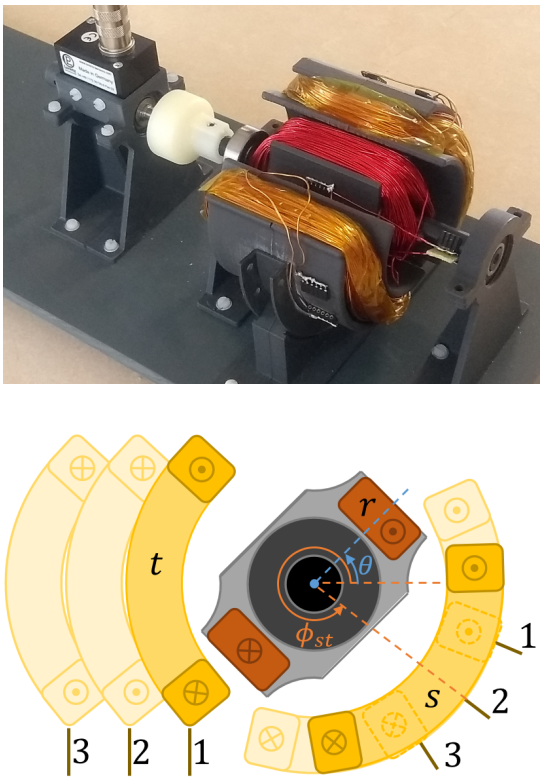

Fig. 1: The experimental setup consists of a transmitter coil (t), a stator resonator (s); and a rotor resonator (r) rotating around an axle. The transmitter distance (d) and the stator orientation (ϕ_{st}) can be changed to three positions each.

200 turns of 0.8 mm wire wound around a curved rectangle with a size of about 8 by 8 cm. The rotor coil also consists of 200 turns of 0.8 mm wire wound around a core with a diameters of 5 cm and a length of 8 cm. Inside the rotor coil, a cylindrical ferrite core was added to improve the coupling with the other coils and to strengthen the magnetic field and thus the torque on the rotor. The ferrite core increases the inductance of the system coils while also slightly increasing their equivalent series resistance due to dissipation in the magnetic material. Table I details the electrical parameter values of the system. Note that the resistance of the coils is highly dependent on the temperature of the copper windings. The resistance values in Table I are hence less accurate in case of having higher electrical currents (and associated torque values).

TABLE I: Transmitter, rotor and stator coil values of the experimental setup depicted in Figure 1 were measured at resonance (6530 Hz).

Parameter	Value
L_t	5.45 mH
R_t	4.5 Ω
R_s	4.5 Ω
R_r	3 Ω

The stator and rotor resonators have a capacitor connected in series with their coils, to compensate their inductance at a certain frequency. This resonance frequency is chosen to maximize the quality factor $\left(Q = \frac{\omega L}{R}\right)$ of the resonators (6530 Hz).

The mutual inductance between the coils was measured by comparing the current in one coil and the induced voltage in the other. Table II shows the measured mutual inductance between transmitter and stator (M_{ts}) for every position. Note that position $M_{ts,13}$ is not physically possible because of the geometry of the coil carriers.

TABLE II: Mutual inductance values of experimental setup (Figure 1) between transmitter and stator (M_{ts}) for all positions and the corresponding transmitter distance (d) and stator orientation (ϕ_{st}).

Mutual inductance		stator position 1	stator position 2	stator position 3	d
transmitter position	1	0.79 mH	0.86 mH	/	0 mm
	2	0.51 mH	0.54 mH	0.59 mH	14 mm
	3	0.40 mH	0.42 mH	0.45 mH	24 mm
ϕ_{st}		5.79 rad	5.60 rad	5.43 rad	

The first harmonic of the mutual inductance profiles between transmitter and rotor (M_{tr}) and between stator and rotor (M_{sr}) were measured and are shown in Figure 2 and Figure 3 respectively. The spatial derivative of the mutual inductance profiles $\left(K_{ab} = \frac{\mathrm{d}M_{ab}(\theta)}{\mathrm{d}\theta}\right)$ can be calculated via numerical differentiation and are indicated by a dashed line. The spatial shifts (ϕ_{st}) between M_{sr} and M_{tr} are listed in Table II.

B. Torque profile validation

The torque profiles were measured for a full rotation of all positions using a Lorenz Messtechnik DR-2112 torque transducer with a nominal torque of 1 Nm ($\pm$ 0.1%). The transmitter voltage was set to 150 V RMS. These measurements are compared against the simulation of the torque profile (2) using the parameters of Table I, and mutual inductance values from Table II and Figures 2 and 3. Measured and simulated torque profiles T_{ij} are shown in Figure 4 for different transmitter positions ($i = 1, 2, 3$) relative to stator positions ($j = 1, 2, 3$). For the simulation, we used the AC resistance values for the coils at room temperature. For higher torques, the increased current in coils raises their ESR values such that the higher

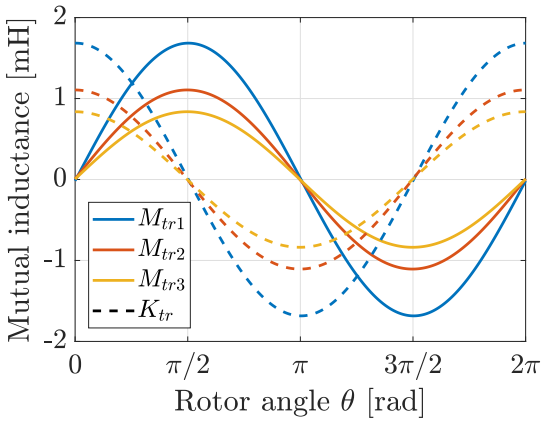

Fig. 2: The mutual inductance between transmitter and rotor (M_{tr}) and its spatial derivative (K_{tr}) were measured on the experimental setup.

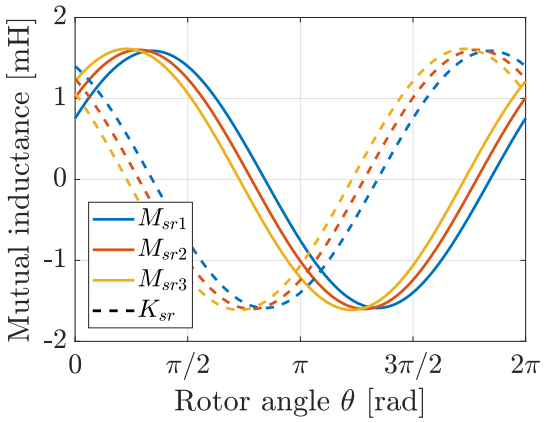

Fig. 3: The mutual inductance between transmitter and rotor (M_{sr}) and its spatial derivative (K_{sr}) were measured on the experimental setup.

torque peaks are slightly overestimated by the simulations. Overall, both the peak torque values and their location are accurately predicted, which validates the model.

IV. Discussion

The torque profile expression (6) can be used to explain the torque profile for the variation in transmitter position (both in distance and orientation). A peak value of the torque is expected for $\sin(\theta - \phi_{st}) = 0$. For this position, the stator and rotor coils are not magnetically coupled. The positional derivative of the stator-rotor coupling (K_{sr}) reaches its peak value for this position. The peaks are however slightly shifted depending on the transmitter distance. This shift is attributed to the variation of the reflected impedance to the transmitter. Equation (3) shows that the reflected impedance reaches its peak value for the same angle ($\phi_{st} = \theta + k\pi$), while Z_r appears in the denominator of (6). Figure 5b shows that the peak values of the total transmitter impedance ($Z_t = R_t + j\omega L_t + Z_r$) coincide with the zero crossings of M_{sr} (Figure 3). The

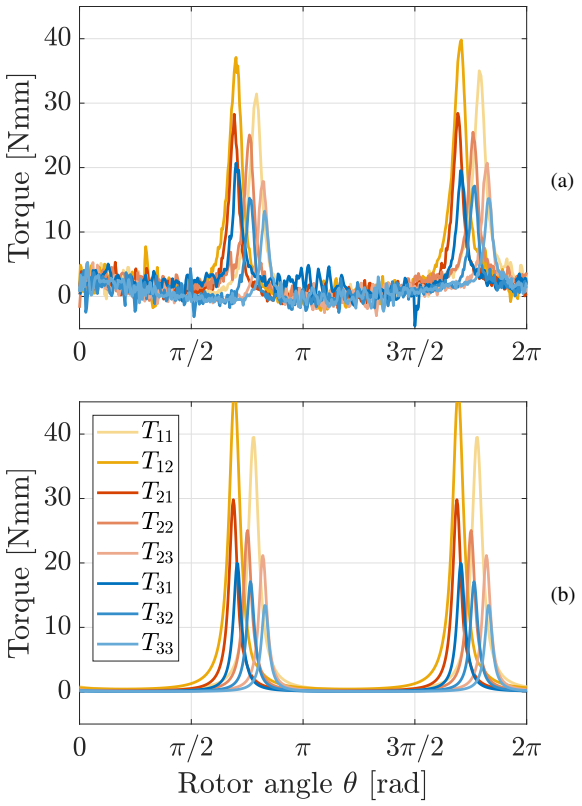

Fig. 4: The measured torque profiles (a) closely resemble the simulated torque profiles (b). The coil resistances are however underestimated in case of relatively higher current amplitudes.

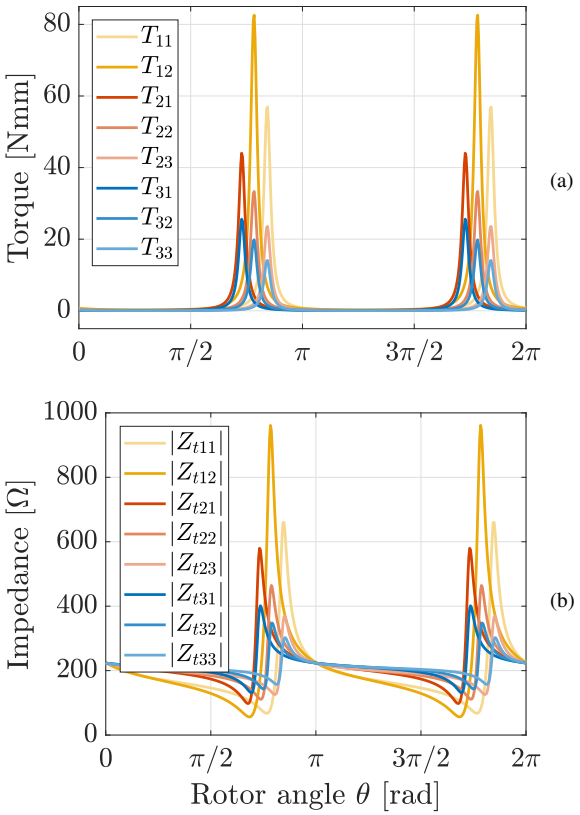

Fig. 5: For a current controlled transmitter (a), the torque peaks correspond to the zero coupling positions between stator and rotor ($M_{sr} = 0; \theta = \phi_{st} + k\pi$). The total transmitter impedance (Z_t) also reaches its peak value for that angle (b). This causes the torque peak to shift to a lower angle θ for a voltage controlled power source.

minimum value of Z_t is located at a slightly lower angle compared to that of the maximum value. For this reason, the torque peak is also shifted to a slightly lower angle. When ignoring the reflected impedance (or in the case of a current controlled transmitter power source), the torque peaks exactly match the zero crossing positions of the stator-rotor coupling. The torque profiles for a current controlled transmitter $\left(\mathrm{i}_t = \dfrac{\mathrm{v}_t}{|R_t + j\omega L_t|}\right)$ are plotted in Figure 5a.

Bringing the transmitter closer to the resonators increases the transmitter-stator coupling (M_{ts}) and the amplitude of the transmitter-rotor coupling ($\mathbb{M}_{tr}$) which in turn increases the torque. Changing the orientation of the stator (ϕ_{st}) shifts M_{sr} sideways. The term $\sin(\phi_{st})$ in (6) suggests that the torque should increase for angles of ϕ_{st} closer to $\frac{3\pi}{2}$. However, the transmitter-stator coupling (M_{ts}) is also strongly affected by the stator orientation. For a transmitter placed at larger distance, M_{ts} would be near zero for $\phi_{st} = \frac{3\pi}{2}$. For the considered system, the transmitter positions are still rather close, such that the stator orientation is limited by the geometry. Lowering the angle ϕ_{st} brings the stator closer to the transmitter and M_{ts} strictly increases when lowering stator orientation ϕ_{st}. Table III shows the measured (exp) and simulated (sim) gain in peak torque when changing the stator orientation from position 1. A gain in torque peak 36-37% was experimentally observed for dedicated transmitter and stator positions. In simulations similar trends were observed. The peak torque gain for transmitter position 3 was again overestimated because because of increasing ESR of the rotor and stator resonators in case of higher induced currents.

TABLE III: Gain in peak torque when changing the stator position (ϕ_{st}) for a given transmitter position.

peak torque gain (sim)		stator position 1	2	3
transmitter position	1	-	18%	/
	2	-	18%	41%
	3	-	28%	49%

peak torque gain (exp)		stator position 1	2	3
transmitter position	1	-	14%	/
	2	-	23%	37%
	3	-	13%	36%

V. Conclusion

By only considering the first spatial harmonic of the mutual inductance profiles M_{tr} and M_{sr}, the torque expression (6) allows us to identify three effects which contribute to the resulting torque profile: (i) For a given current, the torque reaches its peak value when the stator and rotor are not

magnetically coupled ($M_{sr}(\theta) = 0; \theta = \phi_{st} + k\pi$). (ii) For a voltage controlled transmitter power source, the reflected impedance also reaches its peak value around this zero coupling position. This causes the peak torque to shift slightly to a lower rotor angle (θ). (iii) In general, the torque increases when the transmitter is placed closer to the rotor and stator, because M_{ts} and $\mathbb{M}_{tr}$ increase. Bringing ϕ_{st} closer to $\frac{3\pi}{2}$ increases the term $\sin(\phi_{st})$, while also bringing the stator closer to the transmitter. For the considered setup, the stator orientation is geometrically limited, such that M_{ts} increases monotonously when lowering the stator angle ϕ_{st}. A 36% to 37% gain in peak torque was observed when lowering the stator angle to the geometrical limit.

REFERENCES

[1] Grant A Covic and John T Boys. Inductive power transfer. *Proceedings of the IEEE*, 101(6):1276–1289, 2013.

[2] Andre Kurs, Aristeidis Karalis, Robert Moffatt, John D Joannopoulos, Peter Fisher, and Marin Soljačić. Wireless power transfer via strongly coupled magnetic resonances. *science*, 317(5834):83–86, 2007.

[3] Alanson P Sample, David T Meyer, and Joshua R Smith. Analysis, experimental results, and range adaptation of magnetically coupled resonators for wireless power transfer. *IEEE Transactions on Industrial Electronics*, 58(2):544–554, 2011.

[4] Shu Yuen Ron Hui, Wenxing Zhong, and Chi Kwan Lee. A critical review of recent progress in mid-range wireless power transfer. *IEEE Transactions on Power Electronics*, 29(9):4500–4511, 2014.

[5] Olutola Jonah and Stavros V Georgakopoulos. Wireless power transfer in concrete via strongly coupled magnetic resonance. *IEEE Transactions on Antennas and Propagation*, 61(3):1378–1384, 2013.

[6] Xun Liu, WM Ng, CK Lee, and SY Hui. Optimal operation of contactless transformers with resonance in secondary circuits. In *Applied Power Electronics Conference and Exposition, 2008. APEC 2008. Twenty-Third Annual IEEE*, pages 645–650. IEEE, 2008.

[7] Chang-Gyun Kim, Dong-Hyun Seo, Jung-Sik You, Jong-Hu Park, and Bo-Hyung Cho. Design of a contactless battery charger for cellular phone. *IEEE Transactions on Industrial Electronics*, 48(6):1238–1247, 2001.

[8] SY Hui. Planar wireless charging technology for portable electronic products and qi. *Proceedings of the IEEE*, 101(6):1290–1301, 2013.

[9] Ali Abdolkhani, Aiguo Patrick Hu, and Nirmal-Kumar C Nair. A double stator through-hole type contactless slipring for rotary wireless power transfer applications. *IEEE Transactions on Energy Conversion*, 29(2):426–434, 2014.

[10] Siqi Li and Chunting Chris Mi. Wireless power transfer for electric vehicle applications. *IEEE journal of emerging and selected topics in power electronics*, 3(1):4–17, 2015.

[11] Jaegue Shin, Seungyong Shin, Yangsu Kim, Seungyoung Ahn, Seokhwan Lee, Guho Jung, Seong-Jeub Jeon, and Dong-Ho Cho. Design and implementation of shaped magnetic-resonance-based wireless power transfer system for roadway-powered moving electric vehicles. *IEEE Transactions on Industrial Electronics*, 61(3):1179–1192, 2014.

[12] Matthias Vandeputte, Luc Dupré, and Guillaume Crevecoeur. Quasi-static torque profile expressions for magnetic resonance based remote actuation. *IEEE Transactions on Energy Conversion*, 2019.

[13] M Boyvat, C Hafner, and J Leuthold. Wireless control and selection of forces and torques-towards wireless engines. *Scientific reports*, 4:5681, 2014.

[14] Runhong Huang, Bo Zhang, Dongyuan Qiu, and Yuqiu Zhang. Frequency splitting phenomena of magnetic resonant coupling wireless power transfer. *IEEE Transactions on Magnetics*, 50(11):1–4, 2014.